Performance Analysis of A Fiber Optic CDMA LAN Using A Time Domain System Model

Swades K. De[a] and Subrat Kar[b]

[a]Department of Electrical Engineering, State University of New York at Buffalo, NY 14260, USA.

Email: *swadesd@eng.buffalo.edu*

[b]Department of Electrical Engineering, Indian Institute of Technology, New Delhi 110 016, India.

Email: *subrat@ee.iitd.ernet.in*

Abstract

A time domain system model is developed for studying the performance of a FO-CDMA LAN (i) with non-ideal network parameters and (ii) in the presence of multi-user interference (MUI). We examine the effect of chirping in a laser diode on its spectral response. Effects of changes in laser device parameters on its output are studied. Error performance of the complete system, including non-idealities of laser source, optical fiber channel and the APD detector is studied using our time domain simulation model, in the presence of MUI. The effect of having two hard-limiters on the system performance is studied. Our simulation result is verified with the help of an analytical model.

Keywords - Fiber optic CDMA, Time domain system model, Multi-user interference, Optical orthogonal code, Correlation, Synchronous detection.

1 Introduction

To use the vast bandwidth of the optical fiber transmission medium, various different multiaccess schemes have been proposed. Fiber-optic code division multiple access (FO-CDMA) is one such technique which offers an interesting alternative to the other multiple access schemes (*e.g.*, time division multiaccess [TDMA] and wavelength division multiaccess [WDMA]) in some LAN applications, because of its simple network architecture and ease of network access. It is therefore worthwhile to study the performance of such a FO-CDMA network before the actual deployment of the system in the field.

Previously published works on FO-CDMA LAN are mostly analytical[2],[3]. A few authors have carried out investigations on FO-CDMA network components[4],[5],[6],[7]. Work on complete system model using practical parameters has not been done so far. While analytical studies are suitable to predict extreme cases of the system performance, simulation based approaches are helpful in gaining insight into the physical behavior of a system where the necessary assumptions and approximations to model the physical phenomena, needed for analytical studies, are not practical. Our aim is to develop a time domain system model which can reflect non-ideality effects of any of the components on the system performance.

In our system model we consider the passive star topology shown in Fig.1. We consider optical orthogonal codes (OOCs) to encode user data (bit '1's), and use correlation detection process at the receiver end[1]. In general, an (N, W, λ_a, λ_c) optical orthogonal code is a family of $(0,1)$ sequences of length N and weight W with auto- and cross-correlation constraints λ_a and λ_c. In this paper, the family of OOCs considered have $\lambda_a = \lambda_c = 1$. Such a family of OOCs are designated as (N, W, λ_r).

In our simulation model we follow a three tier approach. First, we study the individual functional blocks of the system with practical device and system parameters. Next, we integrate the functional blocks to realize the complete system model. The performance evaluation of the whole

Applications of Photonic Technology 4, Roger A. Lessard, George A. Lampropoulos, Editors, Proceedings of SPIE Vol. 4087 © 2000 SPIE · 0277-786X/00/$15.00

system is carried out at this stage. Finally, we verify the results of our system model using an analytical approach[3].

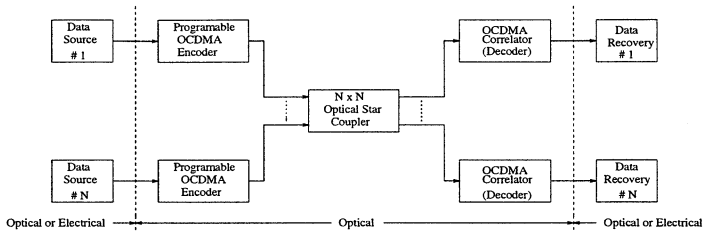

Figure 1: Schematic diagram of a CDMA system with an all-optical encoder and decoder in star configuration

In Section 2, we describe the effects of base current variation of laser diode on its response through its spectral response variation. Effects of variation of device parameters on the laser response are examined here. In Section 3, we examine the system performance of the FO-CDMA LAN using our time domain system model. Simulation results and corresponding analytically calculated values are given in Section 4. A brief outline of the analytical approach of system performance evaluation is also given here. Interpretation of simulation results are presented in Section 5. We conclude our paper in Section 6.

2 Studies on Laser Module

In a LAN, the optical source is almost invariably a direct injection current modulated semiconductor laser diode (SLD). Such a device is always prone to chirping effects, whose time duration may be significant as the chip rate increases i.e. the chip width decreases. We investigate the effect of non-ideal behavior of the SLD on the system performance of the FO-CDMA LAN.

For simulation of laser module we followed the coupled wave analysis. (For details refer to [5],[6].) We determine the knee point of P-I characteristic of SLD before studying the chirping effect in time domain and frequency domain. We also study the effect of SLD device parameter variation on its time domain response.

2.1 P-I Characteristic of SLD

To obtain proper biasing point for the laser operation we study the laser power output versus input injection current (P-I) characteristic. We apply a ramp input current varying from zero to a certain peak value. The simple governing equation for this simulation is

$$I(n) = I_b + \frac{(I_m - I_b)\, n}{N} \tag{1}$$

where I_b is the lower limit of current and I_m is the peak input current, N is the total number of points assumed to be required to reach from I_b to I_m and n varies from 0 to N.

From the P-I characteristics an approximate value of the knee current is determined. With this knowledge of knee current optimum value of I_b and I_m for the input square-pulse injection current (corresponding to binary '1' transmission) is determined, keeping in mind that for a given laser diode $I_b + I_m = I_{mod(max)}$ is constant. A typical square pulse injection current is shown in Fig.2.

2.2 Frequency Response of Chirped SLD Output

Laser response to a current pulse input is stored as discrete data. In discrete time domain, a signal can be represented as the summation of discrete signals, *i.e.*,

$$x = \sum_{k=-\infty}^{+\infty} x(k) \tag{2}$$

where x is possibly an infinite sequence of data.

The Discrete Fourier transform $X(n)$ of the signal $x(k)$ is given by

$$X(n) = F[x(k)] = \sum_{k=-\infty}^{+\infty} x(k)e^{-j2\pi nk} \tag{3}$$

For a signal pulse existing between $k = -N/2$ to $k = +N/2$, Eq.(3) is modified to

$$X(n) = \sum_{-N/2}^{+N/2} x(k)e^{-j2\pi nk} \tag{4}$$

The power spectral density (p.s.d) of the corresponding discrete signal is given by

$$G(n) = \sum_{n=-\infty}^{+\infty} |X(n)|^2 \tag{5}$$

The p.s.d. of the laser pulse output is studied for different combination of I_b and I_m.For different combination of I_b and I_m, we examine the laser chirping from the p.s.d. of laser response.

2.3 SLD Response Characteristics

Laser parameters used to obtain the numerical results are as follows : $\Gamma = 0.3$, $N_o = 10^{24}m^{-3}$, τ_p =3ps, τ_n =1ns, $\beta = 1 \times 10^{-5}$, $V = 1.5 \times 10^{-16}m^3$, $g_o = 2 \times 10^{-12}m^3/s$, $\eta_o = 0.4$, $\lambda_o = 6.25 \times 10^{10}$electron/s, $\varepsilon_s = 1 \times 10^{-23}m^3/s$.

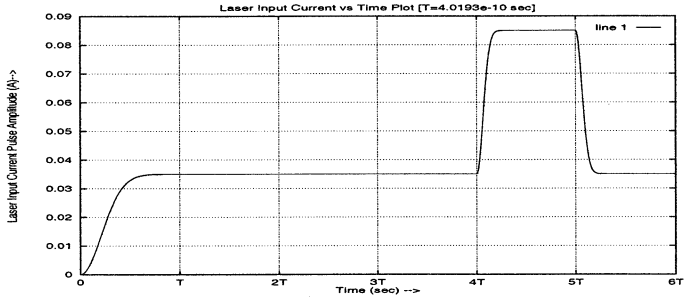

Figure 2: A typical current pulse waveform input to the SLD.

The knee point of P-I characteristic is noted to be around 45mA. Different combinations of (I_b, I_m) are set for the laser modulation input current, keeping the total value, $I_b + I_m$ at a constant value, 85mA. These different combinations of I_b and I_m leads to different values of optical extinction ratio. The SLD output for different (I_b, I_m) combination is plotted in Fig.3. It is observed that when the laser diode is biased below the laser threshold current (*i.e.*, I_b <~45mA, in this case), the relaxation oscillation peak corresponding to the rising edge of modulating signal is much higher, showing a more pronounced chirping effect. As the bias current I_b is increased towards the threshold value (corresponding to the knee of the P-I characteristic of the SLD), the oscillation peak reduces.

The effect of biasing on the spectral response of the laser output signal is shown in Fig.4. From plots (a), (b) and (c), we observe that -

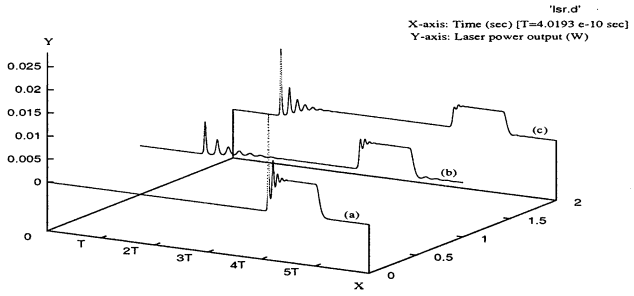

Figure 3: SLD response with different I_b and I_m : (a) with I_b =25mA, I_m =60mA; (b) withI_b =35mA, I_m =50mA; (c) with I_b =45mA, I_m =40mA

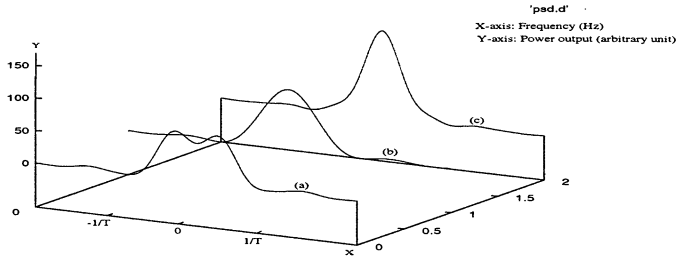

Figure 4: Spectral response of SLD to current pulse input : (a) for I_b =25mA, I_m =60mA; (b) for I_b =35mA, I_m =50mA; (c) for I_b =45mA, I_m =40mA

- For different (I_b, I_m) combinations, the node points of the spectral response remain unchanged
- For biasing current lower than the threshold, the spectral response is more flattened, implying an increase in effective bandwidth requirement.
- The lower the biasing current, the more is the peak amplitude of side lobes of the p.s.d. of signal.

These observations assert that multiuser interference effect will be more for *lower* biasing current. However, it may be pointed out that as the biasing current is increased, the difference between power levels for a mark and a space of a signal reduces (optical extinction ratio reduces), leading to increased probability of error in signal detection. Therefore, there exists an optimum extinction ratio due to the tradeoff between the increased chirp at high extinction ratios and the reduced power level separation between mark and space signals at low extinction ratios[6].

Device parameters are equally important as the biasing parameters to obtain a desired SLD response. We study the effects of variations of gain compression factor, ε_s, mode confinement factor, Γ, fraction of spontaneous emission coupled in the lasing mode, β, differential gain, g_o and electron concentration at transparency, N_o on the laser response. We present here an example of variation of gain compression factor, ε_s.

Noting that the practical range of gain compression factor, ε_s may vary from $1 \times 10^{-23}m^3$ to $5 \times 10^{-23}m^3$, the laser response is studied with three different ε_s: $1 \times 10^{-23}m^3$, $3 \times 19^{-23}m^3$ and $5 \times 10^{-23}m^3$, as shown in Fig.5. It is observed that the relaxation oscillation of SLD get sufficiently reduced, without affecting the peak power output, as we increase the value of ε_s. In view of this it is suggestive that the design parameters of SLD be optimized to achieve higher value of ε_s.

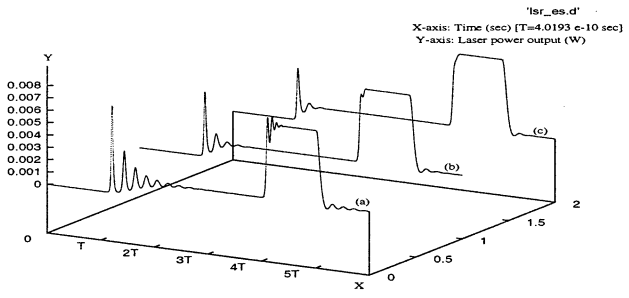

Figure 5: Effect of variation of gain compression factor, ε_s on SLD response : (a) with $\varepsilon_s = 1 \times 10^{-23} m^3$; (b) with $\varepsilon_s = 3 \times 10^{-23} m^3$; (c) with $\varepsilon_s = 5 \times 10^{-23} m^3$

3 The Time Domain System Model

Main functional blocks in a FO-CDMA system are: the light source (SLD), the optical encoder, the fiber optic channel (SMF), the passive optical star coupler, the correlator (optical tapped delay line), the photodetector (APD) and the matched filter receiver. The modules primarily contributing to the system performance are: the SLD, the SMF and the APD detector. In addition to these, MUI is another major player in determining system performance. In this section, we study the system performance of the FO-CDMA LAN through simulation. Non-idealness of system components, *e.g.*, laser chirping, fiber dispersion, photodetector noise, and the effects of MUI are taken into account.

3.1 Device Models

Laser device model and the effects of variation of device parameters on the signal output are examined in Section 2. To develop the system model we consider a suitable set of laser device parameters. We discuss briefly the other device models in a FO-CDMA system.

3.1.1 Fiber Optic Channel

Since in a CDMA system it is required to 'chip' the '1' bit pattern at a very high rate, the overall bit rate of the system is quite high, of the order of a few hundreds of Gbps. Although the length of fiber channel in a LAN application is typically small, due to very high overall bit rate of the system the channel dispersion effect may cause severe BER. Keeping this in view, we consider single mode fiber (SMF) as the transmission channel throughout our study on FO-CDMA LAN. The assumption of SMF is not unrealistic since multi-mode fiber (MMF) runs are limited to a maximum of 0.5 km within a LAN whereas SMFs are used beyond this limits. In a SMF chromatic dispersion is the limiting factor for maximum data rate. For modelling of SMF we assume the fiber loss is wavelength independent and there is no intermodal dispersion. For details of governing equations see [4].

3.1.2 Receiver

In fiber optic LAN applications, a natural choice for the photodetector is the p-i-n diode detector, because in general, such systems are not power constrained and a high receiver sensitivity is not a critical parameter. On the other hand, in FO-CDMA LAN application the signal bit '1' being chopped at high rate and only a few chips per '1' bit being transmitted, the effective energy per bit carried up to the detector end is much lower than the actual bit energy. Such systems are therefore power constrained and, hence, the signal requires amplification at the detection end. The APD, therefore, is a suitable detector in low power applications. Moreover, the internal avalanche

gain of APD detector amplifies the signal during the detection process. With this in view, we have selected the APD as the photodetector in our simulation study of FO-CDMA LAN. We use the APD model based on the acceptance-rejection method developed in [8] to generate random deviates from the WMC p.d.f.

3.1.3 Optical Encoder

The optical encoder module chops the '1' bit into N small time intervals. Out of N chip intervals, only W positions are filled up with pulses, the positions occupied being determined by the desired receiver's address sequence.

The i^{th} baseband signal $s_i(t)$ at the output of the i^{th} optical encoder, is given by[2]

$$s_i(t) = s_i\, b_i(t)\, x_i(t) \tag{6}$$

where s_i, $b_i(t)$, and $x_i(t)$ are the i^{th} user's transmitted optical intensity, binary data signal, and OOC, respectively.

The i^{th} user's binary data signal $b_i(t)$ for continuous communication is given by $b_i(t) = \sum_{j=-\infty}^{+\infty} b_j^{(i)} P_T(t - jT)$, where $b^{(i)} = b_j^{(i)}$ is the i^{th} data sequence that takes on 0 or 1 (OOK) for each j with equal probability and $P_T(t)$ is the rectangular pulse of duration T which starts at $t = 0$. $x_i(t)$, the i^{th} user's OOC, is given by $x_i(t) = \sum_{k=-\infty}^{+\infty} x_k^{(i)} P_{T_c}(t - kT_c)$, where $P_{T_c}(t)$ is the rectangular pulse of duration T_c and $x^{(i)} = x_k^{(i)}$ is the i^{th} periodic sequence of binary optical pulses $(0, +1)$ with period (length) $N = T/T_c$, and weight W.

3.1.4 Optical Correlator Decoder

The optical decoder at the receiver end correlates the received signal with the receiver's own signature sequence to extract the desired information. If the signal (bit '1') carries information for the receiver then an autocorrelation peak results. On the other hand, for '1's for other destination or for '0', low amplitude cross correlation noise results. For modelling the optical correlation detector we adapt the approach given in [2].

3.1.5 Optical Hard-Limiter

The MUI is one major component of system noise which can be reduced by placing an optical hard-limiter (an optical threshold element[9]) before the correlator (optical tapped-delay line)[2],[10]. An ideal optical hard-limiter is a non-linear device which can be defined as

$$g(L) = \begin{cases} v_f & for \quad L \geq v_f \\ 0 & for \quad 0 \leq L < v_f \end{cases} \tag{7}$$

where v_f is the fixed threshold value of the optical hard-limiter dependent on the signal intensity. In our system model, the hard-limiter is taken to be an ideal one, which has the effect of only improving the system performance.

3.2 System Simulation

Our aim here is to study the FO-CDMA LAN performance as a whole through simulation. After testing individual functional modules, namely, the SLD, encoder, SMF, hard-limiter, correlator, APD detector and matched filter receiver, we integrate them together. The system performance evaluation is done from two aspects: first, from the viewpoint of device non-ideality and, second, from the viewpoint of MUI. However, in studying the MUI, device non-idealities were incorporated into the system.

3.2.1 Evolution of Signal at Different Points of the system

To study the evolution of the signal at different points of the FO-CDMA system, following parameters, in addition to the SLD parameters, are considered:

Fiber length: $l = 10km$.

APD detector: quantum efficiency $\eta = 0.8$; gain $G = 4$; dark current $I_d = 10^{-9}A$; carrier ionization ratio $k_{eff} = 0.5$; surface leakage current $I_s = 10nA$; operating wavelength $\lambda = 1550nm$; data rate $R_b = 1/T = 2.5Gbps$; receiver noise temperature $T_r = 1100K$; receiver load resistor $R_l = 1030\Omega$.

OOC: (N, W, λ_r)=(43, 3, 1) (where N is the code length, W is the code weight and λ_r is the correlation coefficient); User codes $\Rightarrow$ {0, 1, 19}, {0, 3, 15}, {0, 4, 13}, {0, 5, 16}, {0, 6, 14}, {0, 7, 17}.

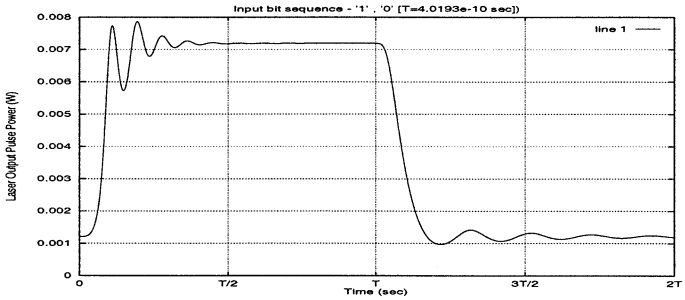

Figure 6: Laser output power corresponding to a current pulse input

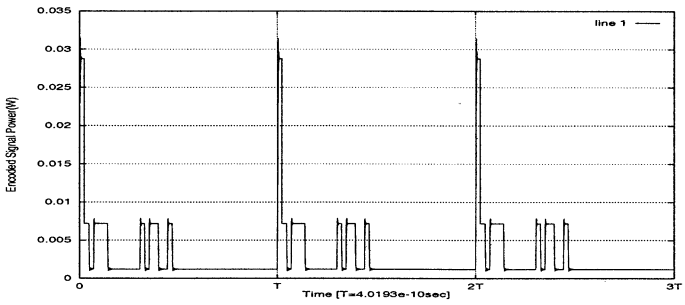

Figure 7: Sum of all user's encoded laser outputs

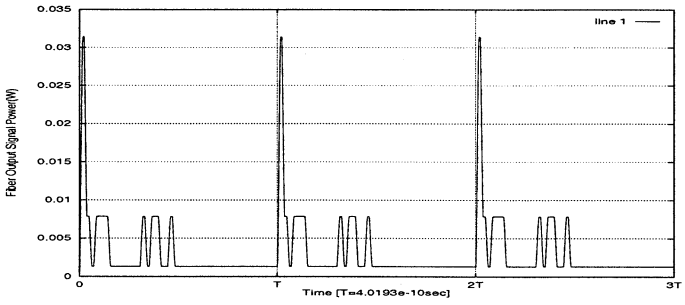

Figure 8: Fiber output corresponding to the encoded signal shown above

Fig.6 shows the laser output pulse corresponding to a bit sequence: '1', '0'. The sum of all users' encoded signals at the fiber input is shown in Fig.7. Corresponding fiber output is shown in Fig.8. In order to examine the dependence of correlation output on the user's code sequence (and hence system performance) we take two receiver outputs: receiver #2 and receiver #4. For

receiver #2 $\{0, 3, 15\}$, the correlator output is shown in Fig.9(a). APD output of receiver #2 is shown in Fig.9(b). For user #4 $\{0, 5, 16\}$, the correlator output and APD output are shown in Fig.10(a) and (b), respectively.

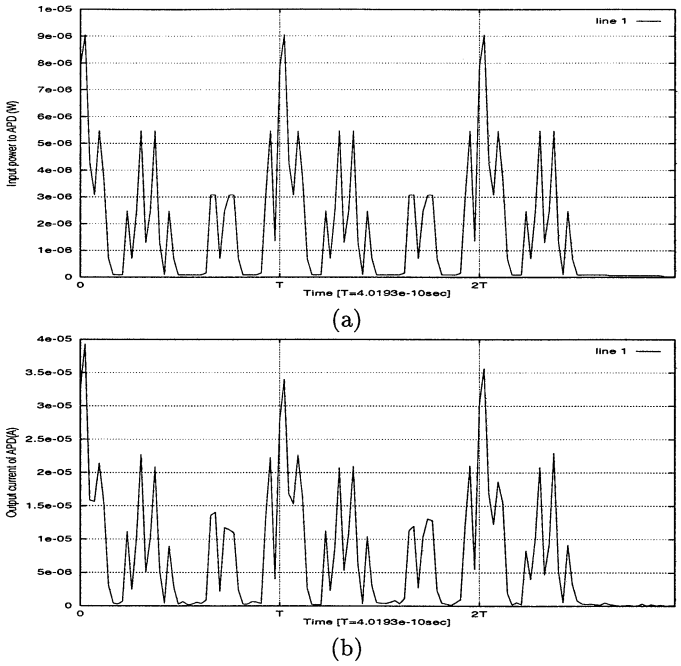

Figure 9: (a) Correlator output of receiver #2 (b) APD response to correlator output

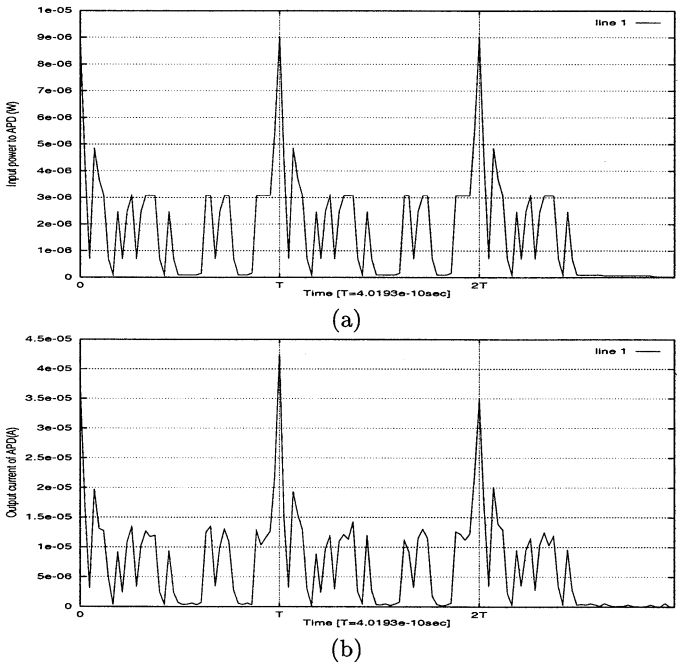

Figure 10: (a) Correlator output of receiver #4 (b) APD response to correlator output

It is observed that the correlation peaks vary randomly at the APD output. It is therefore very crucial to select optimum threshold for achieving minimum BER performance. It is also observed

that correlation output of receiver #2 is affected more by interfering users (higher cross-correlation peaks). This is because of closer proximity of #2 Uer's code with respect to the other interfering user's codes.

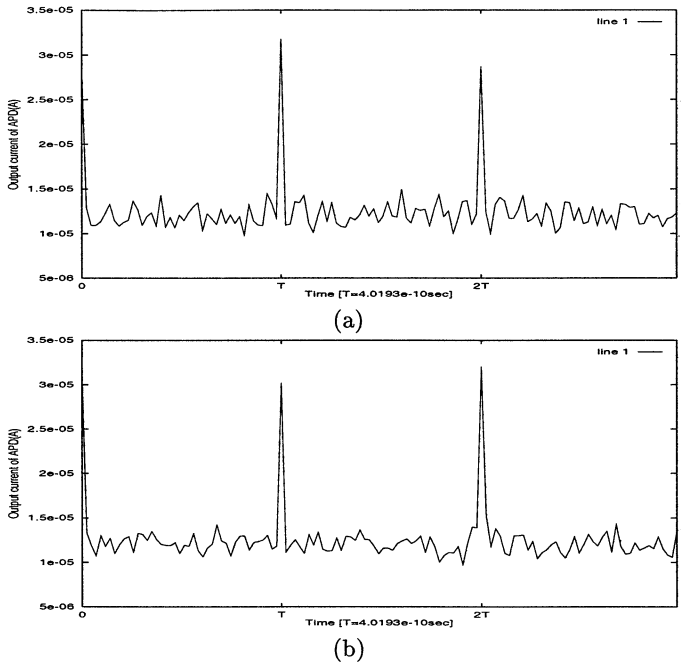

Figure 11: (a) APD response to hard-limited correlator output for receiver #2 (b) APD response to hard-limited correlator output for receiver #4

Fig.11(a) shows the APD output of receiver #2, placing a second hard-limiter after the correlator. For user #4, the corresponding output of APD for receiver is shown in Fig.11(b). It is observed that the signal detection threshold is relaxed, irrespective of the receiver code sequences, if the correlator output is passed through a second hard-limiter, even though the signal power is reduced to some extent. Moreover, the error performance, unlike in earlier case (with single hard-limiter), is much less dependent on the vagaries of the APD detection process.

3.2.2 Effects of MUI

In a CDMA system with OOC sequences the interference level depends on the sequence length N and the code weight W. For a fixed length code, the interference level is lesser for higher values of code weight. Moreover, in these systems the MUI depends on separation among different user's codes. More the separation, lesser is the chance of overlap between two user's codes (*i.e.* weaker is the MUI).

In a chip asynchronous system there is no timing coordination between any two users. Hence the probability of complete overlap of an undesired user's chip on a particular user's chip is less. On the contrary, in a chip synchronous system the probability of overlap of undesired user's chip on the desired user's one is much high. Because of this, chip synchronous systems result in the poorest error performance (upper bound of error probability).

In actual systems, probability of bit error (PE) lies between the two extremes of chip synchronous case and ideal chip asynchronous case[2], *i.e.*,

$$PE(IdealChipAsync) \leq PE(exact) \leq PE(ChipSync) \tag{8}$$

Use of hard-limiter reduces some amount of MUI effects caused by laser chirping and fiber dispersion. But the cross-correlation noise still exists. This is manifested at the output of optical correlator. If the number of users is large and codes are not separated enough, high cross-correlation

noise results. This noise level may reach up to the autocorrelation peak, causing false alarm in the detection process.

By applying a threshold element (a second hard-limiter) at the correlator output the cross-correlation noise level can be reduced to a meager amount. There is a power penalty in this process because of the clipping of power level of autocorrelation peak. Despite this, the bit error probability of the system is reduced to a great extent.

3.2.3 Error Performance of the System in Presence of MUI

To examine the effect of MUI we vary the number of simultaneous users from the minimum to the maximum (in our example, 1 to 6), for the given code length (here, 43), and study the respective error performance. All interfering users are assumed to send bit '1's . Moreover, all the users are assumed to operate in chip synchronous mode[2]. Therefore, the resultant error performance obtained gives the value for the worst possible case.

The whole procedure is repeated for bit '1' and bit '0' to see how the performance varies in these two cases. We suggest the following approaches for estimating actual BER of the FO-CDMA system from the error results.

(A) With Single Hard-Limiter

The hard-limiter is placed before the correlation decoder, to reduce the effect of MUI. Let, with i- active users the number of bits simulated in each case of bit '1' and bit '0' be I_i, and the number of errors for bit '1' and bit '0' transmission by the desired user be n_{1i} and n_{0i}, respectively. Then the error rate for bit '1' transmission in a system of k-users, where k varies from 1 to a U_{max} [see [2], Eq.(16)] is

$$e_{1k} = \sum_{i=1}^{k} \frac{1}{I_i} \frac{n_{1i}}{2^{i-1}}, \tag{9}$$

with the assumption that bit '1' and bit '0' are equiprobable.

The error rate for bit '0' transmission in a system of k-users is

$$e_{0k} = \sum_{i=1}^{k} \frac{1}{I_i} \frac{n_{0i}}{2^{i-1}} \tag{10}$$

From Eqs.(9) and (10), an estimate of BER for a k-user system is given by

$$PE_k[ChipSync] = \frac{1}{2}(e_{1k} + e_{0k}) = \sum_{i=1}^{k} \frac{1}{I_i} \left(\frac{n_{1i} + n_{0i}}{2^i} \right) \tag{11}$$

(B) With Double Hard-Limiter

Second hard-limiter is placed before the APD detector. Since the second hard-limiter reduces the MUI to almost zero, the number of users in the system does not have any impact in its BER performance.

For any number of active users, let, for each case of bit '1' and bit '0', the number iterations performed be I, and the number of bit errors for bit '1' and bit '0' transmission be n_1 and n_0, respectively. Then, an estimate of BER of the system with hard-limiter is given by

$$PE_{HL} = \frac{n_1 + n_0}{2I} \tag{12}$$

Table 1 summarizes the system error performance with single and double hard-limiter, respectively.

4 Verification of Results

To validate our simulation model we adopt the analytical method developed in[3] for chip synchronous system with single hard-limiter.

The conditional bit error probability for a '0' bit transmission is given by

$$P_b\left(Err\,|'0', T_{op}\right) = \frac{1}{2} erfc\left(\frac{T_{op}-\mu_0}{\sqrt{2}\sigma_0}\right) P_{I_1}\left(I_1 = 0\right) + \frac{1}{2}\sum_{j=1}^{U-1}\sum_{m=1}^{min(W,I_1=j)} erfc\left(\frac{T_{op}-\mu_0(m)}{\sqrt{2}\sigma_0(m)}\right).P_{I_1}(j)Pr\left(|i| = m\,|I_1 = j\right) \tag{13}$$

and for a $'1'$ bit transmission, the conditional bit error probability is given by

$$P_b\left(Err\,|'1', T_{op}\right) = \sum_{j=0}^{U-1}\left(1 - \frac{1}{2} erfc\left(\frac{T_{op}-\mu_1}{\sqrt{2}\sigma_1}\right)\right) P_{I_1}(j) \tag{14}$$

From Eqs.(13) and (14) the overall bit error probability is given by

$$P_b = \frac{1}{2}\left\{P_b(Err|'0', T_{op}) + P_b(Err|'1', T_{op})\right\} \tag{15}$$

Following values of system parameters are considered in the analytical model : code parameter $(N, W, \lambda_r) = (43, 3, 1)$; $\{U, T_{op}(\text{photons/chip})\}$=$\{2, 1093\}$, $\{3, 699\}$, $\{4, 535\}$, $\{5, 437\}$ and $\{6, 375\}$ (T_{op} obtained from the threshold power level at the detection end); modulation extinction ratio $M_e = 33.09$ (obtained from the signal waveform at the APD input).

Table 1: Error performance of a FO-CDMA system using single and double hard-limiter, respectively. Code parameters: (N, W, λ_r). Code sequence: $\{0, 1, 19\}, \{0, 3, 15\}, \{0, 4, 13\}, \{0, 5, 16\}, \{0, 6, 14\}, \{0, 7, 17\}$. Receiver power level is approximately $-65dbW$

#Usr	Simulation Results							Analytically obtained BER (single H-L)
	#Smpl	Single H-L			Double H-L			
		#err(1)	#err(0)	Estm BER	#err(1)	#err(0)	Estm BER	
1	10^5	280	0	1.4×10^{-3}	405	29	2.17×10^{-3}	–
2	10^5	1188	3	4.373×10^{-3}	401	24	2.125×10^{-3}	2.459×10^{-4}
3	10^5	5180	441	1.14×10^{-2}	408	26	2.17×10^{-3}	9.464×10^{-3}
4	10^5	12202	4518	2.185×10^{-2}	385	33	2.09×10^{-3}	2.925×10^{-2}
5	10^5	25908	16262	3.503×10^{-2}	398	33	2.155×10^{-3}	5.759×10^{-2}
6	10^5	40112	29028	4.583×10^{-2}	393	26	2.095×10^{-3}	9.082×10^{-2}

5 Remarks

It is observed from columns 5 and 9 in Table 1 that simulation based and analytical error results are of fairly same order. But, for lower number of users the system performance from simulation model is found to be poorer that the analytical prediction. This may be due to the assumption of constant received power level in the simulation model for any number of system users. For smaller number of users, the analytical results predict that the optimum power level is slightly higher.

The system error performance is much poorer than the practical error limit. This is because of the following reasons : (1) The code length considered in our simulation model is 43, whereas in practical systems it is taken to be of the order of 1000. Such a small code length cannot allow different user's codes to be widely separated under the situation when maximum possible users are communicating simultaneously. Moreover, the code weight taken is quite small, which causes larger MUI because of lesser threshold margin at the receiver end. (2) To avoid time complexity of simulation we have considered only chip synchronous case, which gives the poorest system performance. (3) In estimating actual BER it is assumed that probability of bit $'1'$ transmission is 0.5. But in practice this probability is lower than 0.5. Hence, our estimate gives only an upper limit of error performance.

Although the approach is applied here for a chip synchronous FO-CDMA system, and the system error performance in our example is quite poor, this technique of estimating the error performance can be applied generically to any digital system simulation.

6 Conclusion

In this work we have considered the basic FO-CDMA LAN, where the system noise lead to error in detection. No step is taken to recover the bit errors, if it occurs in the system. We suggest a simple approach to estimate the system BER. Validity of the system model is verified with the help of analytical results. Our claim is that the time domain system model can be used as an effective tool for analyzing the system performance by which the impact of any parameter variation can be studied.

References

[1] J. A. Salehi, "Code Division Multiple-Access Techniques in Optical Fiber Networks - Part I : Fundamental Principles," *IEEE Transactions on Communications*, Vol. 37, No. 8, pp. 824-833, Aug. 1989.

[2] J. A. Salehi and C. A. Brackett, "Code Division Multiple-Access Techniques in Optical Fiber Networks - Part II : Systems Performance Analysis," *IEEE Transactions on Communications*, Vol. 37, No. 8, pp. 834-842, Aug. 1989.

[3] H. M. Kwon, "Optical Orthogonal Code-Division Multiple-Access System - Part I : APD Noise and Thermal Noise," *IEEE Transactions on Communications*, Vol. 42, No. 7, pp. 2470-2479, Aug. 1989.

[4] D. G. Duff, "Computer-Aided Design of Digital Lightwave Systems," *IEEE Journal on Selected Areas in Communications,* Vol. 2, No. 1, pp. 171-185, Jan. 1984.

[5] A. F. Elrefie, J. K. Townsend, M. B. Romeiser and K. S. Shanmugan, "Computer Simulation of Digital Lightwave Links," *IEEE Journal on Selected Areas in Communications,* Vol. 6, No. 1, pp. 94-105, Jan. 1988.

[6] J. C. Cartledge and G. S. Burley, "The Effect of Laser Chirping on Lightwave System Performance," *Journal of Lightwave Technology*, Vol. 7, No. 3, pp. 568-573, Mar. 1989.

[7] A. W. Lam and A. M. Hussain, "Performance Analysis of Direct-Detection Optical CDMA Communication Systems with Avalanche Photodiodes," *IEEE Transactions on Communications*, Vol. 40, No. 4, pp. 810-820, Apr. 1992.

[8] J. K. Townsend and K. S. Shanmugan, "On improving the Computational Efficiency of Digital Lightwave Link Simulation," *IEEE Transactions on Communications*, Vol. 38, No. 11, pp. 2040-2048, Nov. 1990.

[9] A. A. Sawchuk and T. C. Strand, "Digital Optical Computing," *Proceedings of IEEE, Special Issue on Optical Computing,* pp. 758-779, Jul. 1984.

[10] T. Ohtsuki, "Performance Analysis of Direct-Detection Optical Asynchronous CDMA Systems with Double Optical Hard-Limiters," *Journal of Lightwave Technology*, Vol. 15, No. 3, pp. 452-457, Mar. 1997.